

Deconfinement transition in protoneutron stars: Analysis within the Nambu–Jona-Lasinio modelG. Lugones,¹ T. A. S. do Carmo,¹ A. G. Grunfeld,^{2,3,4} and N. N. Scoccola^{2,3,5}¹*Universidade Federal do ABC, Centro de Ciências Naturais e Humanas, Rua Santa Adélia, 166, 09210-170, Santo André, Brazil*²*CONICET, Rivadavia 1917, (1033) Buenos Aires, Argentina*³*Departamento de Física, Comisión Nacional de Energía Atómica, (1429) Buenos Aires, Argentina*⁴*Department of Physics, Sultan Qaboos University, P.O. Box: 36 Al-Khode 123 Muscat, Sultanate of Oman*⁵*Universidad Favaloro, Solís 453, (1078) Buenos Aires, Argentina*

(Received 8 January 2010; published 12 April 2010)

We study the effect of color superconductivity and neutrino trapping on the deconfinement transition of hadronic matter into quark matter in a protoneutron star. To describe the strongly interacting matter a two-phase picture is adopted. For the hadronic phase we use different parametrizations of a nonlinear Walecka model which includes the whole baryon octet. For the quark-matter phase we use an $SU(3)_f$ Nambu–Jona-Lasinio effective model which includes color superconductivity. We impose color and flavor conservation during the transition in such a way that just deconfined quark matter is transiently out of equilibrium with respect to weak interactions. We find that deconfinement is more difficult for small neutrino content and it is easier for lower temperatures although these effects are not too large. In addition they will tend to cancel each other as the protoneutron star cools and deleptonizes, resulting a transition density that is roughly constant along the evolution of the protoneutron star. According to these results the deconfinement transition is favored after substantial cooling and contraction of the protoneutron star.

DOI: [10.1103/PhysRevD.81.085012](https://doi.org/10.1103/PhysRevD.81.085012)

PACS numbers: 12.39.Fe, 25.75.Nq, 26.60.Kp

I. INTRODUCTION

It is currently a matter of speculation the actual occurrence of quark matter during protoneutron star (PNS) evolution. The standard scenario for the birth of neutron stars indicates that these objects are formed as consequence of the gravitational collapse and supernova explosion of a massive star [1–3]. Initially, PNSs are very hot and lepton-rich objects, where neutrinos are temporarily trapped. During the first tens of seconds of evolution the PNS evolves to form a cold ($T < 10^{10}$ K) catalyzed neutron star [1–3]. As neutrinos are radiated, the lepton-per-baryon content of matter goes down and the neutrino chemical potential tends to essentially zero in ~ 50 seconds [3]. Deleptonization is fundamental for quark-matter formation inside neutron stars, since it has been shown that the presence of trapped neutrinos in hadronic matter strongly disfavors the deconfinement transition [4,5]. In fact, neutrino trapping makes the density for the deconfinement transition to be higher than in the case of neutrino-free hadronic matter. As a consequence, the transition could be delayed several seconds after the bounce of the stellar core. However, the calculations presented in [4,5] were performed employing the MIT bag model for the description of quark matter and did not include the effect of color superconductivity. As we shall see in the present work, the use of the Nambu–Jona-Lasinio (NJL) model and the inclusion of color superconductivity may change qualitatively the effect of neutrino trapping in the deconfinement conditions.

As emphasized in earlier works [4–11], an important characteristic of the deconfinement transition in neutron stars, is that just deconfined quark matter is transiently out

of equilibrium with respect to weak interactions. In fact, depending on the temperature, the transition should begin with the quantum or thermal nucleation of a small quark-matter drop near the center of the star. On the other hand, the flavor composition of hadronic matter in β equilibrium is different from that of a β -stable quark-matter drop. Roughly speaking, the direct formation of a β -stable quark drop with N quarks will need the almost simultaneous conversion of $\sim N/3$ up and down quarks into strange quarks, a process which is strongly suppressed with respect to the formation of a non β -stable drop by a factor $\sim G_{\text{Fermi}}^{2N/3}$. For typical values of the critical-size β -stable drop ($N \sim 100\text{--}1000$ [6]) the suppression factor is actually tiny. Thus, quark flavor must be conserved during the deconfinement transition [4–10]. When color superconductivity is included together with flavor conservation, the most likely configuration of the just deconfined phase is two-flavor color superconducting (2SC) provided the pairing gap is large enough [9]. The relevance of this 2SC intermediate phase (a kind of activation barrier) has been analyzed for deleptonized neutron stars [10,12] but not for hot and lepton-rich objects like PNSs.

In the present paper we shall analyze the deconfinement transition in protoneutron star conditions employing the Nambu–Jona-Lasinio model in the description of quark matter. For the hadronic phase we shall use a model based on a relativistic Lagrangian of hadrons interacting via the exchange of σ , ρ , and ω mesons [13]. For simplicity, the analysis will be made in bulk, i.e. without taking into account the energy cost due to finite size effects in creating a drop of deconfined quark matter in the hadronic environment.

The present article is organized as follows. In Sec. II we present the main aspects of the nonlinear Walecka model describing the hadronic phase. In Sec. III we present the generalities of the model we use for the quark phase. In Sec. IV we show our numerical results and finally in Sec. V we discuss our results and present the conclusions.

II. THE HADRONIC PHASE

For the hadronic phase we shall use a nonlinear Walecka model (NLWM) [13–16] which includes the whole baryon octet, electrons, and electron neutrinos in equilibrium under weak interactions. The Lagrangian of the model is given by

$$\mathcal{L} = \mathcal{L}_B + \mathcal{L}_M + \mathcal{L}_L, \quad (1)$$

where the indices B , M , and L refer to baryons, mesons, and leptons, respectively. For the baryons we have

$$\begin{aligned} \mathcal{L}_B = \sum_B \bar{\psi}_B [\gamma^\mu (i\partial_\mu - g_{\omega B} \omega_\mu - g_{\rho B} \vec{\tau} \cdot \vec{\rho}_\mu) \\ - (m_B - g_{\sigma B} \sigma)] \psi_B, \end{aligned} \quad (2)$$

with $B = n, p, \Lambda, \Sigma^+, \Sigma^0, \Sigma^-, \Xi^-, \text{ and } \Xi^0$. The contribution of the mesons σ , ω , and ρ is given by

$$\begin{aligned} \mathcal{L}_M = \frac{1}{2} (\partial_\mu \sigma \partial^\mu \sigma - m_\sigma^2 \sigma^2) - \frac{b}{3} m_N (g_\sigma \sigma)^3 - \frac{c}{4} (g_\sigma \sigma)^4 \\ - \frac{1}{4} \omega_{\mu\nu} \omega^{\mu\nu} + \frac{1}{2} m_\omega^2 \omega_\mu \omega^\mu - \frac{1}{4} \vec{\rho}_{\mu\nu} \cdot \vec{\rho}^{\mu\nu} \\ + \frac{1}{2} m_\rho^2 \vec{\rho}_\mu \cdot \vec{\rho}^\mu, \end{aligned} \quad (3)$$

where the coupling constants are $g_{\sigma B} = x_{\sigma B} g_\sigma$, $g_{\omega B} = x_{\omega B} g_\omega$, and $g_{\rho B} = x_{\rho B} g_\rho$. The ratios $x_{\sigma B}$, $x_{\omega B}$, and $x_{\rho B}$ are equal to 1 for the nucleons and acquire different values for the other baryons depending on the parametrization (see Table I). The leptonic sector is included as a free Fermi gas of electrons and electron neutrinos in chemical equilibrium with the other particles.

There are five constants in the model that are determined by the properties of nuclear matter, three that determine the nucleon couplings to the scalar, vector, and vector-isovector mesons g_σ/m_σ , g_ω/m_ω , g_ρ/m_ρ , and two that determine the scalar self-interactions b and c . It is assumed that all hyperons in the octet have the same coupling than the Λ . These couplings are expressed as a ratio to the nucleon couplings mentioned above, that we thus simply denote x_σ , x_ω , and x_ρ . In the present work we use two

parametrizations for the constants. One of them is the standard parametrization GM1 given by Glendenning-Moszkowski [13], as shown in Table I. This parametrization employs ‘‘low’’ values for x_σ , x_ω , and x_ρ . The parametrization GM4 employs larger values of these couplings. This makes the EOS stiffer and increases the maximum mass of hadronic stars to $2.2M_\odot$; see Table I.

The derivation of the equations describing the model is given in detail in [17]. The total pressure P and mass-energy density ρ are given by

$$\begin{aligned} P = \sum_{i=B,L} P_i + \frac{1}{2} \left(\frac{g_\omega}{m_\omega} \right)^2 \rho_B'^2 - \frac{1}{2} \left(\frac{g_\sigma}{m_\sigma} \right)^{-2} (g_\sigma \sigma)^2 \\ - \frac{1}{3} b m_n (g_\sigma \sigma)^3 - \frac{1}{4} c (g_\sigma \sigma)^4 + \frac{1}{2} \left(\frac{g_\rho}{m_\rho} \right)^2 \rho_{I_3}^2, \end{aligned} \quad (4)$$

$$\begin{aligned} \rho = \sum_{i=B,L} \rho_i + \frac{1}{2} \left(\frac{g_\omega}{m_\omega} \right)^2 \rho_B'^2 + \frac{1}{2} \left(\frac{g_\sigma}{m_\sigma} \right)^{-2} (g_\sigma \sigma)^2 \\ + \frac{1}{3} b m_n (g_\sigma \sigma)^3 + \frac{1}{4} c (g_\sigma \sigma)^4 + \frac{1}{2} \left(\frac{g_\rho}{m_\rho} \right)^2 \rho_{I_3}^2. \end{aligned} \quad (5)$$

Here P_i and ρ_i are the expressions for a Fermi gas of relativistic, noninteracting particles:

$$P_i = \frac{1}{3} \frac{g_i}{(2\pi)^3} \int d^3 p \frac{p^2}{(p^2 + m_i^{*2})^{1/2}} (f_i(T) + \bar{f}_i(T)), \quad (6)$$

$$\rho_i = \frac{g_i}{(2\pi)^3} \int d^3 p (p^2 + m_i^{*2})^{1/2} (f_i(T) + \bar{f}_i(T)), \quad (7)$$

where $f_i(T)$ and $\bar{f}_i(T)$ are the Fermi-Dirac distribution functions for particles and antiparticles, respectively:

$$f_i(T) = (\exp([(p^2 + m_i^{*2})^{1/2} - \mu_i^*]/T) + 1)^{-1}, \quad (8)$$

$$\bar{f}_i(T) = (\exp([(p^2 + m_i^{*2})^{1/2} + \mu_i^*]/T) + 1)^{-1}. \quad (9)$$

Note that for baryons we use, instead of masses m_i and chemical potentials μ_i , ‘‘effective’’ masses m_i^* and chemical potentials μ_i^* given by

$$m_i^* = m_i + x_{\sigma i} (g_\sigma \sigma), \quad (10)$$

$$\mu_i^* = \mu_i - x_{\omega i} \left(\frac{g_\omega}{m_\omega} \right)^2 \rho_B' - x_{\rho i} I_{3i} \left(\frac{g_\rho}{m_\rho} \right)^2 \rho_{I_3}', \quad (11)$$

where I_{3i} is the third component of the isospin of each baryon.

TABLE I. Parameters of the hadronic equation of state. For each parametrization we give the maximum mass M_{\max} of a hadronic star.

Label	Composition	$x_\sigma = x_\rho$	x_ω	$(g_\sigma/m_\sigma)^2$ [fm ²]	$(g_\omega/m_\omega)^2$ [fm ²]	$(g_\rho/m_\rho)^2$ [fm ²]	b	c	M_{\max}
GM 1	baryon octet + e^-	0.6	0.653	11.79	7.149	4.411	0.002 947	-0.001 070	$1.78M_\odot$
GM 4	baryon octet + e^-	0.9	0.9	11.79	7.149	4.411	0.002 947	-0.001 070	$2.2M_\odot$

The weighted isospin density ρ'_{I_3} and the weighted baryon density ρ'_B are given by

$$\rho'_{I_3} = \sum_{i=B} x_{\rho i} I_{3i} n_i, \quad (12)$$

$$\rho'_B = \sum_{i=B} x_{\omega i} n_i, \quad (13)$$

where n_i is the particle number density of each baryon:

$$n_i = \frac{g_i}{(2\pi)^3} \int d^3 p (f_i(T) - \bar{f}_i(T)). \quad (14)$$

The mean field $g_\sigma \sigma$ satisfies the equation

$$\left(\frac{g_\sigma}{m_\sigma}\right)^{-2} (g_\sigma \sigma) + b m_n (g_\sigma \sigma)^2 + c (g_\sigma \sigma)^3 = \sum_{i=B} x_{\sigma i} n_i^s, \quad (15)$$

where n_i^s is the scalar density:

$$n_i^s = \frac{g_i}{(2\pi)^3} \int d^3 p \frac{m_i^*}{(p^2 + m_i^{*2})^{1/2}} (f_i(T) + \bar{f}_i(T)). \quad (16)$$

The hadron phase is assumed to be charge neutral and in chemical equilibrium under weak interactions. Electric charge neutrality states

$$n_p + n_{\Sigma^+} - n_{\Sigma^-} - n_{\Xi^-} - n_e = 0. \quad (17)$$

Chemical weak equilibrium in the presence of trapped electron neutrinos implies that the chemical potential μ_i of each baryon in the hadron phase is given by

$$\mu_i = q_B \mu_n - q_e (\mu_e - \mu_{\nu_e}), \quad (18)$$

where q_B is its baryon charge and q_e is its electric charge. For simplicity we are assuming that muon and tau neutrinos are not present in the system, and their chemical potentials are set to zero.

All the above equations can be solved numerically by specifying three thermodynamic quantities, e.g. the temperature T , the mass-energy density ρ , and the chemical potential of electron neutrinos in the hadronic phase $\mu_{\nu_e}^H$.

III. THE QUARK-MATTER PHASE

In order to study the just deconfined quark-matter phase we use an $SU(3)_f$ NJL effective model which also includes color superconducting quark-quark interactions. The corresponding Lagrangian is given by

$$\begin{aligned} \mathcal{L} = & \bar{\psi}(i\not{\partial} - \hat{m})\psi + G \sum_{a=0}^8 [(\bar{\psi}\tau_a\psi)^2 + (\bar{\psi}i\gamma_5\tau_a\psi)^2] \\ & + 2H \sum_{A,A'=2,5,7} [(\bar{\psi}i\gamma_5\tau_A\lambda_{A'}\psi_C)(\bar{\psi}Ci\gamma_5\tau_A\lambda_{A'}\psi)], \end{aligned} \quad (19)$$

where $\hat{m} = \text{diag}(m_u, m_d, m_s)$ is the current mass matrix in flavor space. In what follows we will work in the isospin symmetric limit $m_u = m_d = m$. Moreover, τ_i and λ_i with

$i = 1, \dots, 8$ are the Gell-Mann matrices corresponding to the flavor and color groups, respectively, and $\tau_0 = \sqrt{2}/31_f$. Finally, the charge conjugate spinors are defined as follows: $\psi_C = C\bar{\psi}^T$ and $\bar{\psi}_C = \psi^T C$, where $\bar{\psi} = \psi^\dagger \gamma^0$ is the Dirac conjugate spinor and $C = i\gamma^2 \gamma^0$.

To be able to determine the relevant thermodynamical quantities we have to obtain the grand canonical thermodynamical potential at finite temperature T and chemical potentials μ_{fc} . Here, $f = (u, d, s)$ and $c = (r, g, b)$ denotes flavor and color indices, respectively. For this purpose, starting from Eq. (19), we perform the usual bosonization of the theory. This can be done by introducing scalar and pseudoscalar meson fields σ_a and π_a , respectively, together with the bosonic diquark field Δ_A . In this work we consider the quantities obtained within the mean field approximation (MFA). Thus, we only keep the non-vanishing vacuum expectation values of these fields and drop the corresponding fluctuations. For the meson fields this implies $\hat{\sigma} = \sigma_a \tau_a = \text{diag}(\sigma_u, \sigma_d, \sigma_s)$ and $\pi_a = 0$. Concerning the diquark mean field, we will assume that in the density region of interest only the 2SC phase might be relevant. Thus, we adopt the ansatz $\Delta_5 = \Delta_7 = 0$, $\Delta_2 = \Delta$. Integrating out the quark fields and working in the framework of the Matsubara and Nambu-Gorkov formalism we obtain the following MFA quark thermodynamical potential (a detailed procedure of calculation can be found in Refs. [18–21]):

$$\begin{aligned} \Omega_q^{\text{MFA}}(T, \mu_{fc}, \sigma_u, \sigma_d, \sigma_s, |\Delta|) = & \frac{1}{\pi^2} \int_0^\Lambda dk k^2 \sum_{i=1}^9 \omega(x_i, y_i) \\ & + \frac{1}{4G} (\sigma_u^2 + \sigma_d^2 + \sigma_s^2) \\ & + \frac{|\Delta|^2}{2H}, \end{aligned} \quad (20)$$

where Λ is the cutoff of the model and $\omega(x, y)$ is defined by

$$\begin{aligned} \omega(x, y) = & -[x + T \ln[1 + e^{-(x-y)/T}] \\ & + T \ln[1 + e^{-(x+y)/T}]], \end{aligned} \quad (21)$$

with

$$\begin{aligned} x_{1,2} = E, \quad x_{3,4,5} = E_s, \\ x_{6,7} = \sqrt{\left[E + \frac{(\mu_{ur} \pm \mu_{dg})}{2}\right]^2 + \Delta^2}, \\ x_{8,9} = \sqrt{\left[E + \frac{(\mu_{ug} \pm \mu_{dr})}{2}\right]^2 + \Delta^2}, \quad y_1 = \mu_{ub}, \\ y_2 = \mu_{db}, \quad y_3 = \mu_{sr}, \quad y_4 = \mu_{sg}, \quad y_5 = \mu_{sb}, \\ y_{6,7} = \frac{(\mu_{ur} - \mu_{dg})}{2}, \quad y_{8,9} = \frac{(\mu_{ug} - \mu_{dr})}{2}. \end{aligned} \quad (22)$$

Here, $E = \sqrt{k^2 + M^2}$ and $E_s = \sqrt{k^2 + M_s^2}$, where $M_f = m_f + \sigma_f$. Note that in the isospin limit we are working $\sigma_u = \sigma_d = \sigma$ and, thus, $M_u = M_d = M$.

The total thermodynamical potential of the quark-matter phase (QMP) is obtained by adding to Ω_{MFA} the contribution of the leptons. Namely,

$$\begin{aligned}\Omega_{\text{QMP}}(T, \mu_{fc}, \mu_e, \mu_{\nu_e}, \sigma, \sigma_s, |\Delta|) \\ = \Omega_q^{\text{MFA}}(T, \mu_{fc}, \sigma, \sigma_s, |\Delta|) + \Omega_e(T, \mu_e) \\ + \Omega_{\nu_e}(T, \mu_{\nu_e}) - \Omega_{\text{vac}},\end{aligned}\quad (23)$$

where Ω_e and Ω_{ν_e} are the thermodynamical potentials of the electrons and neutrinos, respectively. For them we use the expression corresponding to a free gas of ultrarelativistic fermions,

$$\Omega_l(T, \mu_l) = -\gamma_l \left(\frac{\mu_l^4}{24\pi^2} + \frac{\mu_l^2 T^2}{12} + \frac{7\pi^2 T^4}{360} \right), \quad (24)$$

where $l = e, \nu_e$ and the degeneracy factor is $\gamma_e = 2$ for electrons and $\gamma_{\nu_e} = 1$ for neutrinos. Notice that in Eq. (23) we have subtracted the constant Ω_{vac} in order to have a vanishing pressure at vanishing temperature and chemical potentials.

From the grand thermodynamic potential Ω_{QMP} we can readily obtain the pressure $P = -\Omega_{\text{QMP}}$, the number density of quarks of each flavor and color $n_{fc} = -\partial\Omega_{\text{QMP}}/\partial\mu_{fc}$, the number density of electrons $n_e = -\partial\Omega_{\text{QMP}}/\partial\mu_e$, and the number density of electron neutrinos $n_{\nu_e} = -\partial\Omega_{\text{QMP}}/\partial\mu_{\nu_e}$. The corresponding number densities of each flavor, n_f , and of each color, n_c , in the quark phase are given by $n_f = \sum_c n_{fc}$ and $n_c = \sum_f n_{fc}$, respectively. The baryon number density reads $n_B = \frac{1}{3}\sum_{fc} n_{fc} = (n_u + n_d + n_s)/3$. Finally, the Gibbs free energy per baryon is

$$g_{\text{quark}} = \frac{1}{n_B} \left(\sum_{fc} \mu_{fc} n_{fc} + \mu_e n_e + \mu_{\nu_e} n_{\nu_e} \right). \quad (25)$$

For the NJL model we use two sets of constants shown in Table II. The sets 1 and 2 were taken from [22,23], respectively, but without the 't Hooft flavor mixing interaction. The procedure, obtained from [24] is to keep Λ and m fixed, then tune the remaining parameters G and m_s in order to reproduce $M = 367.6$ MeV and $M_s = 549.5$ MeV at zero temperature and density. The resulting parameter sets are given in Table II. For these sets of parameters we get $\Omega_{\text{vac}} = -4301$ MeV/fm³ and $\Omega_{\text{vac}} = -5099$ MeV/fm³ (for set 1 and 2, respectively). It should be noticed that, following [24], it is possible to define a quantity B which plays a role similar to that of the ‘‘bag constant in the MIT bag model.’’ Namely, B corresponds to

the difference between the pressure of the interacting quark matter and that of the free one, both taken at vanishing temperature and chemical potential. It is important to stress, however, that in the present model B should not be considered as an extra parameter since its value is calculable once the model parameters are fixed. In our case we obtained $B = 353$ MeV/fm³ for set 1 and 337.2 MeV/fm³ for set 2, which are within the range of values quoted in Table 2.2 of Ref. [24].

In order to derive a quark-matter equation of state (EOS) from the above formulas it is necessary to impose a suitable number of conditions on the variables $\{\mu_{fc}\}$, μ_e , μ_{ν_e} , σ , σ_s , and Δ . Three of these conditions are consequences from the fact that the thermodynamically consistent solutions correspond to the stationary points of Ω with respect to σ , σ_s , and Δ . Thus, we have

$$\partial\Omega_{\text{QMP}}/\partial\sigma = 0, \quad \partial\Omega_{\text{QMP}}/\partial\sigma_s = 0, \quad \partial\Omega_{\text{QMP}}/\partial|\Delta| = 0. \quad (26)$$

To obtain the remaining conditions one must specify the physical situation in which one is interested in. As in previous works [4–10], we are dealing here with just deconfined quark matter that is temporarily out of chemical equilibrium under weak interactions. The appropriate condition in this case is flavor conservation between hadronic and deconfined quark matter. This can be written as

$$Y_f^H = Y_f^Q, \quad f = u, d, s, e, \nu_e, \quad (27)$$

with $Y_f^H \equiv n_f^H/n_B^H$ and $Y_f^Q \equiv n_f^Q/n_B^Q$ being the abundances of each particle in the hadron and quark phase, respectively. In other words, the just deconfined quark phase must have the same ‘‘flavor’’ composition than the β -stable hadronic phase from which it has been originated. Notice that, since the hadronic phase is assumed to be electrically neutral, flavor conservation ensures automatically the charge neutrality of the just deconfined quark phase. The conditions given in Eq. (27) can be combined to obtain

$$\begin{aligned}n_d = \xi n_u, \quad n_s = \eta n_u, \quad n_{\nu_e} = \kappa n_u, \\ 3n_e = 2n_u - n_d - n_s,\end{aligned}\quad (28)$$

where n_i is the particle number density of the i species in the quark phase. The quantities $\xi \equiv Y_d^H/Y_u^H$, $\eta \equiv Y_s^H/Y_u^H$, and $\kappa \equiv Y_{\nu_e}^H/Y_u^H$ are functions of the pressure and temperature, and they characterize the composition of the hadronic phase. These expressions are valid for *any* hadronic EOS. For hadronic matter containing n , p , Λ , Σ^+ , Σ^0 , Σ^- , Ξ^- , and Ξ^0 , we have

$$\xi = \frac{n_p + 2n_n + n_\Lambda + n_{\Sigma^0} + 2n_{\Sigma^-} + n_{\Xi^-}}{2n_p + n_n + n_\Lambda + 2n_{\Sigma^+} + n_{\Sigma^0} + n_{\Xi^0}}, \quad (29)$$

$$\eta = \frac{n_\Lambda + n_{\Sigma^+} + n_{\Sigma^0} + n_{\Sigma^-} + 2n_{\Xi^0} + 2n_{\Xi^-}}{2n_p + n_n + n_\Lambda + 2n_{\Sigma^+} + n_{\Sigma^0} + n_{\Xi^0}}, \quad (30)$$

TABLE II. The two sets of NJL parameters.

	$m_{u,d}$ [MeV]	m_s [MeV]	Λ [MeV]	$G\Lambda^2$	H/G
Set 1	5.5	112.0	602.3	4.638	3/4
Set 2	5.5	110.05	631.4	4.370	3/4

$$\kappa = \frac{n_{\nu_e}^H}{2n_p + n_n + n_\Lambda + 2n_{\Sigma^+} + n_{\Sigma^0} + n_{\Xi^0}}. \quad (31)$$

Additionally, the deconfined phase must be locally colorless; thus it must be composed by an equal number of red, green, and blue quarks:

$$n_r = n_g = n_b. \quad (32)$$

Also, ur , ug , dr , and dg pairing will happen provided that $|\Delta|$ is nonzero, leading to

$$n_{ur} = n_{dg}, \quad n_{ug} = n_{dr}. \quad (33)$$

In order to have all Fermi levels at the same value, we consider [9]

$$n_{ug} = n_{ur}, \quad n_{sb} = n_{sr}. \quad (34)$$

These two equations, together with Eqs. (32) and (33) imply that $n_{ur} = n_{ug} = n_{dr} = n_{dg}$ and $n_{sr} = n_{sg} = n_{sb}$ [9].

Finally, including the conditions Eqs. (26) we have 13 equations involving the 14 unknowns (σ , σ_s , $|\Delta|$, μ_e , μ_{ν_e} , and $\{\mu_{fc}\}$). For given value of one of the chemical potentials (e.g. μ_{ur}), the set of equations can be solved once the values of the parameters ξ , η , κ , and the temperature T are given. Instead of μ_{ur} , we can provide a value of the Gibbs free energy per baryon g_{quark} or the pressure P and solve simultaneously Eqs. (28)–(34) together with Eq. (26) in order to obtain σ , σ_s , $|\Delta|$, μ_e , μ_{ν_e} , and $\{\mu_{fc}\}$.

IV. DECONFINEMENT TRANSITION IN PROTONEUTRON STAR MATTER

In order to determine the transition conditions, we apply the Gibbs criteria, i.e. we assume that deconfinement will occur when the pressure and Gibbs energy per baryon are the same for both hadronic matter and quark matter at a given common temperature. Thus, we have

$$g^H = g^Q, \quad P^H = P^Q, \quad T^H = T^Q, \quad (35)$$

where the index H refers to hadron matter and the index Q to quark matter. According to these conditions (together with the equations of Secs. II and III), for a given temperature T^H and neutrino chemical potential of the trapped neutrinos in the hadronic phase $\mu_{\nu_e}^H$, there is a unique pressure P at which the deconfinement is possible. Instead of P , we may characterize the transition point by giving the Gibbs free energy per baryon g , or alternatively, the mass-energy density of the hadronic phase ρ_H (see Figs. 1–3). We emphasize that, according to the present description, P and g are the same in both the hadronic phase and the just deconfined phase. However, the mass-energy density ρ_H and ρ_Q at the transition point are different in general. Similarly, while the abundance Y_{ν_e} of neutrinos is the same in both the hadronic and just deconfined quark phases, the chemical potentials $\mu_{\nu_e}^Q$ and $\mu_{\nu_e}^H$ are different.

According to numerical simulations [1–3], during the first tens of seconds of evolution the protoneutron star

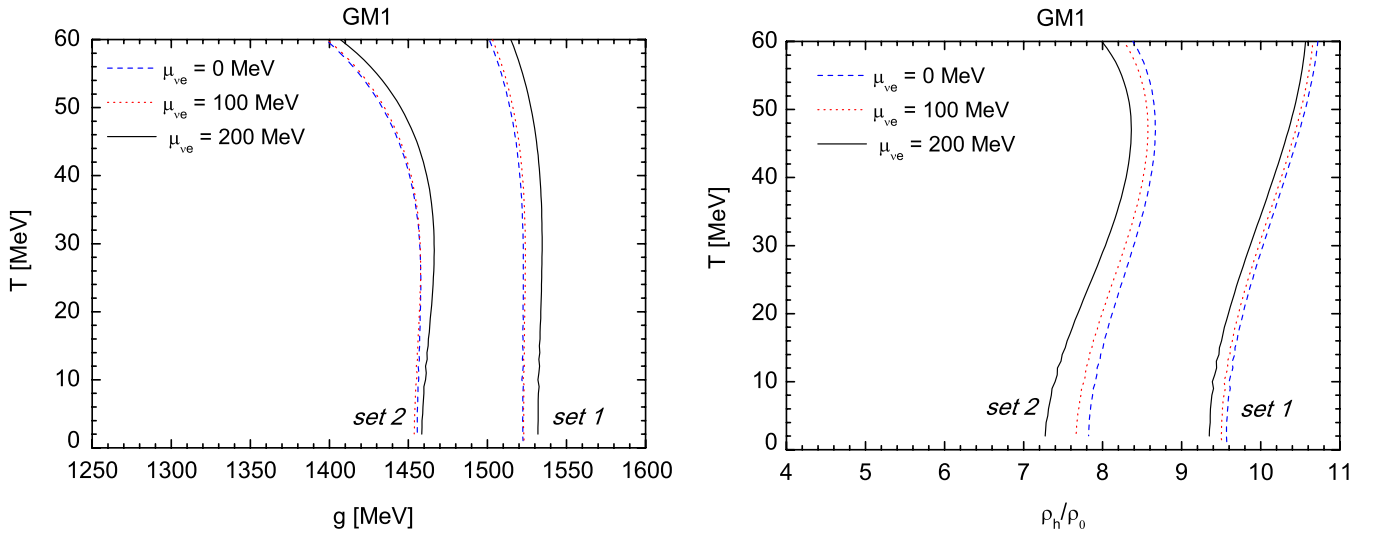


FIG. 1 (color online). *Left panel*: the Gibbs free energy density per baryon g at which deconfinement occurs versus the temperature T for three different values of the neutrino chemical potential in the hadronic phase ($\mu_{\nu_e}^H = 0$ MeV in dashed line, $\mu_{\nu_e}^H = 100$ MeV in dotted line, and $\mu_{\nu_e}^H = 200$ MeV in solid line). *Right panel*: the mass-energy density of the hadronic phase at which deconfinement occurs versus the temperature T , for the same values of $\mu_{\nu_e}^H$ given in the left panel (density is given in units of the nuclear saturation density ρ_0). The hadronic phase is described by the GM1 parametrization of the EOS. For the quark phase we adopt the two parametrizations of the NJL model given in Table II. In both panels, if the thermodynamic state of hadronic matter (characterized by $\{T^H, g^H, \mu_{\nu_e}^H\}$ or by $\{T^H, \rho_H, \mu_{\nu_e}^H\}$) lies to the left of the curve corresponding to the same $\mu_{\nu_e}^H$, then the deconfinement transition is not possible. In the right side region of a given curve the preferred phase is deconfined quark matter.

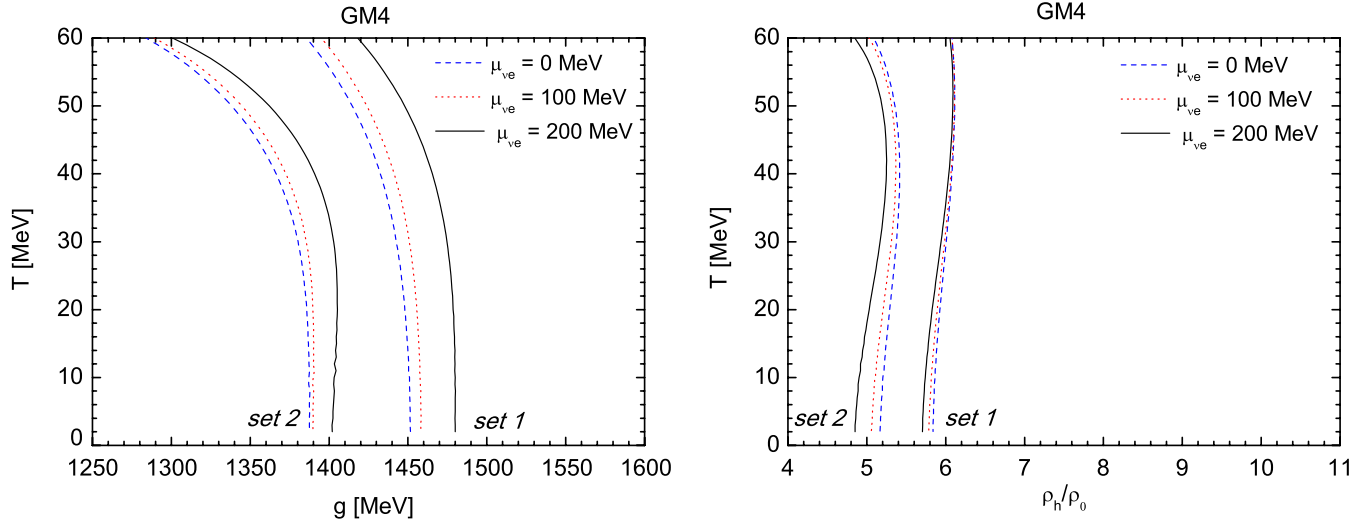


FIG. 2 (color online). Same as Fig. 1 but employing the GM4 parametrization of the hadronic equation of state.

cools from $T \sim 40$ MeV to temperatures below 2–4 MeV. In the same period, the chemical potential $\mu_{\nu_e}^H$ of the trapped neutrinos evolves from ~ 200 MeV to essentially zero. Thus, in order to consider typical PNS conditions we have solved Eqs. (35) together with the equations of Secs. II and III for temperatures in the range 0–60 MeV and $\mu_{\nu_e}^H$ in the range 0–200 MeV. The results are displayed in Figs. 1–3 for all the parametrizations of the equations of state given in previous sections.

In Fig. 1 we display the results for the GM1 parametrization of the hadronic EOS. In the left panel of Fig. 1 we show the Gibbs free energy density per baryon g at which

deconfinement occurs versus the temperature T for three different values of the neutrino chemical potential in the hadronic phase ($\mu_{\nu_e}^H = 0, 100, 200$ MeV). In the right panel the same results are shown but as a function of the mass-energy density of the hadronic phase (in units of the nuclear saturation density $\rho_0 = 2.7 \times 10^{14}$ g cm $^{-3}$). In both figures, if the thermodynamic state of hadronic matter (characterized, e.g., by T^H , ρ_H , and $\mu_{\nu_e}^H$) lies to the left of the curve, corresponding to the same $\mu_{\nu_e}^H$, then the deconfinement transition is not possible. In the right side region of a given curve the preferred phase is deconfined quark matter. Notice that the transition's Gibbs free energy

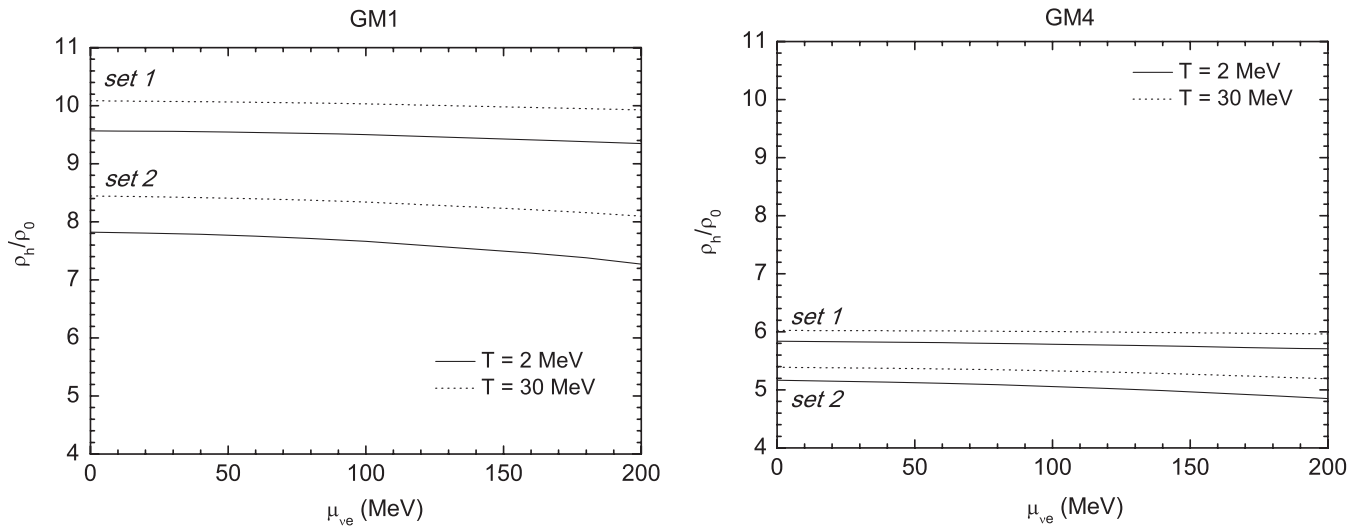


FIG. 3. The mass-energy density of the hadronic phase at which deconfinement occurs as a function of the chemical potential of trapped neutrinos $\mu_{\nu_e}^H$. Results are given for two temperatures: $T = 2$ MeV in solid line and $T = 30$ MeV in dashed line. We employed the GM1 (left panel) and the GM4 (right panel) parametrization of the hadronic EOS. Notice that there is a small decrease of the transition density ρ_h for large $\mu_{\nu_e}^H$.

is an increasing function of $\mu_{\nu_e}^H$. However, the transition density of the hadronic phase slightly decreases as $\mu_{\nu_e}^H$ increases. In Fig. 2 we display the results for the GM4 parametrization of the hadronic EOS. The results are qualitatively the same but the transition densities are smaller than those for GM1 by $\sim 30\%$.

Notice that in Figs. 1 and 2 we have employed the Gibbs free energy per baryon g defined in Eq. (25). The baryon number chemical potential μ_B and the quark number chemical potential μ are usually employed in the QCD phase diagram. The baryon number chemical potential μ_B is defined in a similar way than g but it does not include the contribution of leptons. The quark number chemical potential μ is defined as $\mu_B/3$. Since the contribution of leptons is not dominant in our case we have $g \approx \mu_B = 3\mu$. In fact, we have verified numerically that for the physical conditions found in Figs. 1 and 2 the difference between g and μ_B never exceeds a 5%.

In Fig. 3 we show the behavior of the transition's density as a function of the chemical potential of trapped neutrinos $\mu_{\nu_e}^H$ for two specific temperatures ($T = 2$ and 30 MeV). It is clearly seen that for a fixed temperature the effect of deleptonization is to inhibit the transition. This effect is not very large; at fixed temperature there is a slight increase by less than a 10% when $\mu_{\nu_e}^H$ falls from 200 MeV to 0 MeV. On the other hand, the effect of cooling works in the opposite direction because pairing tends to help the transition and the gap increases as the temperature goes down. The effect of cooling is also small; at fixed $\mu_{\nu_e}^H$ there is a slight decrease of the transition density ρ_H by less than a 10% when the temperature falls from 30 MeV to 2 MeV. Both effects tend to cancel each other as the PNS cools and deleptonizes, resulting a transition density that is roughly constant along the evolution of the protoneutron star.

V. CONCLUSIONS

In this paper we have investigated the role of color superconductivity in the deconfinement transition from hadronic matter to quark matter at finite temperature and in the presence of a trapped neutrino gas. The study presented here is relevant for the first tens of seconds of evolution of newly born protoneutron stars.

In our analysis we used a two-phase description where we employed the Nambu–Jona-Lasinio model in the description of quark matter (Sec. III) and a nonlinear Walecka model which includes the whole baryon octet, electrons, and electron neutrinos in equilibrium under weak interactions in the description of hadronic matter (Sec. II). Deconfinement is assumed to be a first order phase transition and the just deconfined quark phase is assumed to have the same “flavor composition” than the β -stable hadronic phase from which it has been originated (see [12] and references therein). When color superconductivity is included together with flavor conservation [9],

the most likely configuration of the just deconfined phase is 2SC provided the pairing gap is large enough (we are not considering here the possible role of inhomogeneous superconductive phases [25]). This just deconfined phase is out of chemical equilibrium under weak interactions and thus it is very short lived but it is a kind of “activation barrier” that determines the onset of the deconfinement transition.

The main result of the present paper is that, within the NJL model, deconfinement is more difficult for small neutrino content and it is easier for lower temperatures. This effect is not very large, at least for the here-used parametrizations of the NJL model. At fixed temperature there is a slight increase by less than a 10% when $\mu_{\nu_e}^H$ falls from 200 MeV to 0 MeV (see Fig. 3). The effect of cooling is also small; at fixed $\mu_{\nu_e}^H$ there is a slight decrease of the transition density ρ_H by less than a 10% when the temperature falls from 30 MeV to 2 MeV (see Fig. 3). This is due to the fact that the pairing gap becomes larger as the temperature decreases and therefore the increase of the condensation term favors the transition at low temperatures. Both effects tend to cancel each other as the PNS cools and deleptonizes, resulting a transition density that is roughly constant along the evolution of the protoneutron star.

The here-found behavior is qualitatively opposite to what it was found within the MIT bag model. In fact, previous analysis without including the effect of color superconductivity [4,5] show that the presence trapped neutrinos pushes up the transition density to values much larger than for neutrino-free matter. It was also found in [4,5] that the transition is easier for larger temperatures. More recent results including the effect of color superconductivity within the MIT bag model [26] show that the transition density increases with neutrino trapping but (in coincidence with the here-found results) the pairing gap favors the transition as the temperature decreases.

In spite of some differences between the results within the NJL and the MIT bag model description of quark matter some general conclusions may be obtained about the effect of color superconductivity in the deconfinement transition. First, when color superconductivity is present the deconfinement density is not so strongly affected by neutrino trapping as it is in the unpaired case. Second, color superconductivity makes the transition easier at lower temperatures and the dependence of the deconfinement density with T is much smaller than in the unpaired case.

During cooling and deleptonization of the protoneutron star the temperature and the chemical potential of trapped neutrinos fall abruptly in a few seconds and there is also some contraction of the whole neutron star. It is interesting to note that although the density increase is not too large, it may be comparatively important for the deconfinement transition because the effects of temperature and neutrino

trapping are smoothed by color superconductivity. According to our results the deconfinement transition is favored after substantial cooling and contraction of the protoneutron star but full numerical simulations of protoneutron star evolution are needed in order to determine whether and when the deconfinement conditions are attained.

ACKNOWLEDGMENTS

This work was supported in part by CONICET (Argentina) Grant No. PIP 6084 and by ANPCyT (Argentina) Grant No. PICT07 03-00818. T. A. S. do Carmo acknowledges the financial support received from UFABC (Brazil). G. Lugones acknowledges the financial support received from FAPESP and CNPq (Brazil).

-
- [1] A. Burrows and J.M. Lattimer, *Astrophys. J.* **307**, 178 (1986).
 - [2] W. Keil and H.-Th. Janka, *Astron. Astrophys.* **296**, 145 (1995).
 - [3] J. A. Pons *et al.*, *Astrophys. J.* **513**, 780 (1999).
 - [4] G. Lugones and O.G. Benvenuto, *Phys. Rev. D* **58**, 083001 (1998).
 - [5] O. G. Benvenuto and G. Lugones, *Mon. Not. R. Astron. Soc.* **304**, L25 (1999).
 - [6] K. Iida and K. Sato, *Phys. Rev. C* **58**, 2538 (1998).
 - [7] M.L. Olesen and J. Madsen, *Phys. Rev. D* **49**, 2698 (1994).
 - [8] I. Bombaci, I. Parenti, and I. Vidaña, *Astrophys. J.* **614**, 314 (2004).
 - [9] G. Lugones and I. Bombaci, *Phys. Rev. D* **72**, 065021 (2005).
 - [10] I. Bombaci, G. Lugones, and I. Vidaña, *Astron. Astrophys.* **462**, 1017 (2007).
 - [11] I. Bombaci, D. Logoteta, P.K. Panda, C. Providencia, and I. Vidana, *Phys. Lett. B* **680**, 448 (2009)
 - [12] G. Lugones, A.G. Grunfeld, N.N. Scoccola, and C. Villavicencio, *Phys. Rev. D* **80**, 045017 (2009).
 - [13] N. K. Glendenning and S. A. Moszkowski, *Phys. Rev. Lett.* **67**, 2414 (1991).
 - [14] J.D. Walecka, *Ann. Phys. (N.Y.)* **83**, 491 (1974); B. D. Serot and J.D. Walecka, *Adv. Nucl. Phys.* **16**, 1 (1986).
 - [15] J. Boguta and A.R. Bodmer, *Nucl. Phys.* **A292**, 413 (1977).
 - [16] D.P. Menezes and C. Providência, *Phys. Rev. C* **68**, 035804 (2003); A.M.S. Santos and D.P. Menezes, *Phys. Rev. C* **69**, 045803 (2004).
 - [17] N. K. Glendenning, *Astrophys. J.* **293**, 470 (1985).
 - [18] M. Huang, P.f. Zhuang, and W. q. Chao, *Phys. Rev. D* **67**, 065015 (2003).
 - [19] S.B. Ruester, V. Werth, M. Buballa, I. A. Shovkovy, and D.H. Rischke, *Phys. Rev. D* **72**, 034004 (2005).
 - [20] D. Blaschke, S. Fredriksson, H. Grigorian, A.M. Oztas, and F. Sandin, *Phys. Rev. D* **72**, 065020 (2005).
 - [21] M. Ciminale, R. Gatto, N.D. Ippolito, G. Nardulli, M. Ruggieri, *Phys. Rev. D* **77**, 054023 (2008).
 - [22] P. Rehberg, S.P. Klevansky, and J. Hufner, *Phys. Rev. C* **53**, 410 (1996).
 - [23] T. Hatsuda and T. Kunihiro, *Phys. Rep.* **247**, 221 (1994).
 - [24] M. Buballa, *Phys. Rep.* **407**, 205 (2005).
 - [25] R. Casalbuoni and G. Nardulli, *Rev. Mod. Phys.* **76**, 263 (2004).
 - [26] T. A. S. do Carmo and G. Lugones (unpublished).